JOURNAL OF PROPULSION AND POWER
Vol. 12, No. 4, July–August 1996

Evolution of Internal Flow in a Solid Rocket Motor with Radial Slots

Jayant S. Sabnis*
United Technologies Research Center, East Hartford, Connecticut 06108
and
Mark A. Eagar†
United Technologies Chemical Systems Division, San Jose, California 95135

A study of the internal flow in a solid rocket motor with radial slots was conducted via numerical solution of Reynolds-averaged Navier–Stokes equations. The main objective of this effort was to study the internal flow structure with regard to its implications on the flow-induced instabilities. Two different radial slot designs were considered under the present study. The first configuration considered represents a conventional radial slot design, wherein the forward and the aft faces of the slot are in planes normal to the motor axis. The second radial slot design studied under this effort was designed with the slot faces curved toward the aft direction and a contoured aft-corner. The contoured slot design was aimed at providing a better aerodynamic flow-path to turn the slot flow toward the nozzle, thereby resulting in a flowfield that would be less susceptible to instabilities. The computed results obtained for conventional slot design indicate that there is flow separation near the aft edge of the slot. The simulation results obtained for the contoured slot design indicate that this design is quite successful in eliminating the aft-corner flow separation and, results in a more stable flow structure. The internal flow calculations for the motor with this contoured slot design were conducted at several different web-burn conditions. These simulations show that the evolution of the flowfield structure in the slot cavity with the web burn can vary significantly depending upon the axial location of the slot. The flowfield in the aft slot cavity of the three-slot motor studied under the present effort evolved initially to resemble a driven cavity flow. At subsequent burn-back geometry, the flow in this slot evolved to resemble the flow over a backward facing step. The flow structure in the forward and the center slots of this motor shows no similar evolution.

Introduction

THE internal flow in solid rocket motors (SRM) has significant impact upon ballistics, stability, grain structural integrity, and the thermal protection system. The erosive burning phenomenon controlled by the internal flow affects the motor ballistics. Regions of flow separation and shear layers in the internal flowfield affect the motor stability. The pressure distribution at the grain surface, determined by the internal flow, is a key factor in determining the instantaneous stresses in the grain. Similarly, the structure of the boundary layers near the motor case and nozzle control the heat load, and hence, determine the thermal protection requirements. The structure of the internal flowfield depends strongly on the motor port geometry. The present work was aimed at studying the internal flow in motors with radial slots.

For a radial slot design, the flow in the vicinity of the slot exit is always of particular interest. The slot flow can result in the formation of a low-pressure region downstream of the slot, depending upon the ratio of the slot flow momentum to the bore flow momentum. This low-pressure region can result in substantial loads on the propellant grain resulting in undesirable grain deformation leading to catastrophic results. Such undesirable interaction between the internal flow and the propellant grain structural deformation has been identified as the cause of Castor II motor failure by Glick et al.[1] The same phenomenon has also resulted in the failure of the Titan SRMU PQM-1 motor. The low-pressure region downstream of the slot also results in adverse pressure gradient along the propellant surface, and can create a region of reversed flow at the grain surface. This phenomenon has been observed previously by Sabnis et al.[2] The reversed flow region results in a velocity profile with higher propensity to motor instability. The port geometry in a radial slot grain undergoes significant changes through the motor burn. The radial slots evolve into a cavity-like shape as the slots get wider during the motor burn. This could significantly alter the internal flow structure in the vicinity of the slots. Thus, a motor design that is stable initially could show increased propensity to instability later in the burn. The evolution of the internal flowfield structure and its implications on the motor stability (not the flow-structural interaction) in solid rocket motors with radial slots is the focus of this article.

Flow-induced instabilities can be caused by the presence of regions of reversed flow as well as shear layers that can shed vortices. Vortices shed from shear layers result in increased blockage as they pass through the throat, thereby generating pressure oscillations. Flow structure in the vicinity of reversed flow regions tends to be sensitive to pressure perturbations. This sensitivity can alter the heat transfer to the propellant surface, thereby affecting the burn rate. Hence, these flowfield features need to be minimized as far as possible. An improved understanding of the flow structure in the motor port during the motor operation is of significant importance in the design of solid rocket motors. A study of the internal flow structure at several web burn conditions using experimental techniques is likely to be prohibitively expensive. However, analytical tools using computational fluid dynamics (CFD) techniques can be effectively used in such studies. Numerical solution of

Received July 7, 1994; revision received Jan. 8, 1996; accepted for publication Feb. 2, 1996.

*Principal Research Engineer, M/S 129-20, 411 Silver Lane. Senior Member AIAA.
†Ballistics Engineer. Member AIAA.

ensemble-averaged Navier–Stokes equations has been utilized by several researchers recently in view of the generality of this approach, and recent advances in numerical techniques as well as the digital computers. Multidimensional numerical analyses have been developed to simulate single-phase, nonreacting flow (see, e.g., Sabnis et al.[2] and Chang[3]), two-phase nonreacting flow (see, e.g., Madabhushi et al.[4] and Golafshani and Loh[5]), as well as two-phase reacting flow (see Sabnis et al.[6]). The computer resources required for a three-dimensional, multiphase, reacting flow Navier–Stokes calculation may render it impractical for use in SRM design analysis. However, CFD can be used effectively in the analysis of specific design related issues. Such efforts require identification of the flow physics important to the specific issue and then using CFD to analyze the relevant flow physics. The present study was aimed at demonstrating such a judicious use of CFD in the evaluation of design concepts for a solid rocket motor with radial slots.

Analysis and Simulation Technique

The simulation of the internal flow in selected radial slot geometric configurations was conducted under the present effort via a numerical solution of Reynolds-averaged Navier–Stokes equations. The turbulence model used in the study was the two-equation k-ε turbulence model of Jones and Launder[7] with the modifications of Sabnis et al.[8] for solid rocket internal flows. The CFD code used for the numerical simulations is the CELMINT code developed for simulation of solid rocket internal flows under a U.S. Air Force Phillips Laboratory contract.[9] The CELMINT code utilizes a consistently split, linearized block-implicit (LBI) numerical scheme developed by Briley and McDonald.[10] The LBI scheme for scalar convection and diffusion in two space dimensions does not suffer from a stability restriction that relates the temporal step to the spatial mesh size. This is an important advantage, apparently retained for the present system of equations, in view of the existence of high characteristic velocities, and the need to use locally refined meshes for accurate solution of the flowfield equations in the regions of sharp velocity, temperature, or species concentration gradients. Further, the solution procedure treats the nonlinearities noniteratively by Taylor series linearization in time, and then splitting the matrix into a sequence of easily solved block-banded subsystems. The solution procedure is computationally efficient. The LBI algorithm has been found to be rapidly convergent and conditionally stable in three dimensions for nonperiodic inflow and outflow boundary conditions. Details of the stability and convergence rate of the algorithm have been discussed by Briley et al.[11]

The CELMINT code can be used for internal flow simulation including two-phase and distributed aluminum combustion effects. Since the objective of the present effort was the gas-phase flowfield structure, the two-phase and chemistry effects were not included in the interest of reduced requirements for computing resources. An equivalent gas-particle mixture (EGPM) assumption was used for the propellant gas. Details of the governing equations in the CELMINT code can be found in the publications cited previously (Refs. 2, 6, and 9).

The boundary conditions used with the continuous-phase governing equations were as follows. The head end and the nozzle walls were considered adiabatic and chemically inert. Hence, the velocity components and the normal derivatives of enthalpy at these walls were set to zero. The nozzle exit boundary is a supersonic outflow boundary (except in the boundary layer). Hence, all of the dependent variables at this boundary were linearly extrapolated (i.e., the second derivative along the axial direction was set to zero). At the propellant surface, the gas-phase mass flux was determined from the propellant burn rate and the temperature was determined by the adiabatic flame temperature for the propellant formulation.

Test Cases and Results

The motor geometry chosen as the test case under the present study was one with a port length-to-diameter ratio $L/D \approx 31$ (at ignition) and three radial slots. This design allows the study of flowfield structure in the vicinity of slots with three significantly different values of slot-to-bore flow momentum ratio. Two different radial slot designs were considered under the present study. The first configuration, shown schematically in Fig. 1, represents a conventional radial slot design. The slot faces are in a plane normal to the motor axis in this configuration. The flow in the slot is, therefore, directed radially inward. At the slot exit, the slot flow has to turn toward the aft direction, which results in acceleration of the gas and reducing the static pressure. As the gas slows down subsequently, the static pressure increases, resulting in a region of adverse pressure gradient along the axial direction at the propellant surface aft of the slot exit. Since this adverse pressure gradient can result in flow reversal, the flowfield has a higher propensity for instabilities. It should be possible to significantly reduce (and even eliminate) the flow reversal near the slot exit by contouring the slot surface so as to provide a better aerodynamic surface to turn the slot flow toward the nozzle. To examine this concept, a part of the present effort was aimed at studying the internal flowfield in an alternate slot design that has the potential to avoid these problems.

A modified radial slot design (shown in Fig. 2), where the slots were curved toward the aft direction and the aft-corner of the slot was contoured, was conceived. This design would provide a better aerodynamic surface for the slot flow to accomplish the radial-to-axial turning. The contoured corner results in controlled acceleration of the slot flow as it is turned along the axial direction. This avoids the possibility of overacceleration of the flow around the edge, followed by deceleration that results in the adverse pressure gradient at the grain surface.

Conventional Radial Slot Design Analysis

The conventional radial slot design was analyzed using the geometry corresponding to the ignition condition for this motor. At these conditions, the L/D for the motor grain port was approximately 31. The forward, center, and the aft radial slots were located at about 7, 13, and 23 diameters from the head end, respectively. The slot width for all slots was 32% of the port diameter, whereas the grain web thickness was 1.1 times the port diameter. The computational grid used in these calculations consisted of 80 grid points along the radial direction and 450 grid points along the axial direction. The grid spacing in the near-wall region was sufficiently fine to resolve the viscous sublayer. Typical value of $\Delta r/R$ at the propellant surface was 10^{-4}, while corresponding value for inert surfaces was 10^{-5}. This grid resolution was sufficient to get the first grid point from the surface within $y^+ < 5$.

Calculations were conducted using an IBM RS/6000 model 370 workstation. Converged solutions were obtained in approximately 3000 iterations that required about 16 h to complete. The streamlines for the flow in the vicinity of the forward slot have been presented in Fig. 3. This figure shows the reversed flow region present near the aft corner at the slot exit. The flowfield at the center and the aft slot exit is qualitatively similar. However, the ratio of the slot flow momentum to that of the bore flow decreases from forward to aft slot. Hence, the size of the reversed flow region could be observed to decrease from the forward to the aft slot.

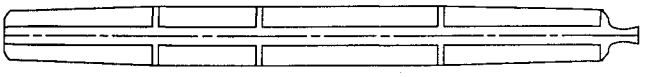

Fig. 1 Schematic diagram of conventional radial slot motor.

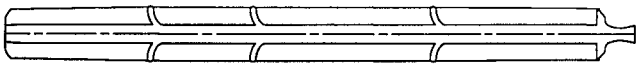

Fig. 2 Schematic diagram of aft-curved radial slot motor.

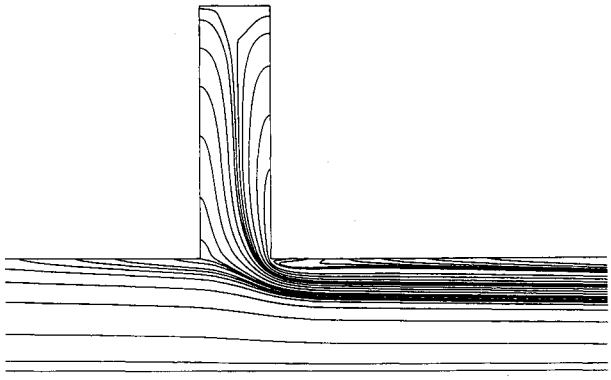

Fig. 3 Streamlines for flow near forward slot at ignition (conventional radial slot design).

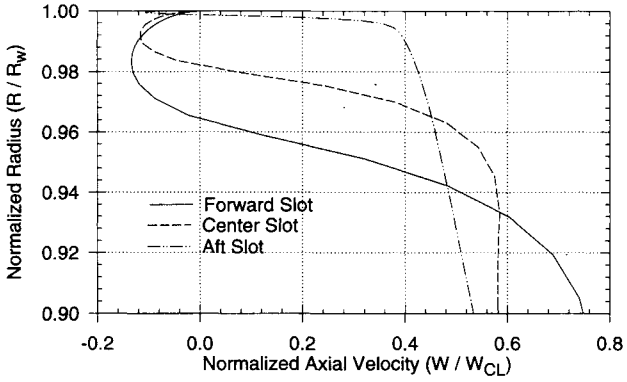

Fig. 4 Normalized axial velocity profiles at slot exit for conventional radial slot grain.

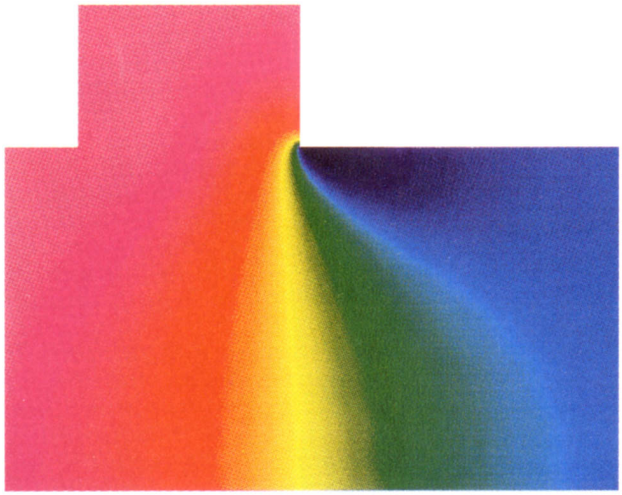

Fig. 5 Pressure distribution near forward slot exit (conventional radial slot design).

The normalized axial velocity profiles immediately downstream of the three slots are shown in Fig. 4. As can be observed from these plots, the inflection in the velocity profile renders the flowfield susceptible to instabilities since this results in reduced damping associated with disturbance modes. The static pressure distribution near the exit of the forward slot is presented in Fig. 5. This figure shows the low-pressure region that exists near the propellant surface at the slot exit and can produce undesirable grain deformation.

Aft-Curved Radial Slot Design Analysis

In view of the undesirable features of the flowfield near the slot exit for a conventional radial slot design, the modified radial slot design with aft-curved slots (shown in Fig. 2) was conceived. The curvature in this slot design helps to turn the slot flow in the aft direction. Furthermore, the contoured surface at the aft corner of the slot was designed to provide a better aerodynamic surface for radial-to-axial turning of the slot flow. The aerodynamic surface results in controlled acceleration of the slot flow as it is turned along the axial direction. This avoids the possibility of overacceleration of the flow around the edge, followed by deceleration that results in the adverse pressure gradient at the grain surface along the axial direction. Eliminating the adverse pressure gradient will avoid flow reversal at the grain surface. To examine the flowfield structure with the aft-curved radial slots, the internal flow calculations were conducted at the ignition geometry for this grain design. The slot geometry was chosen so that the total surface area in the slot with the aft-curved slot grain was identical to that with the conventional radial slot grain. The computational grid utilized in these calculations was similar to the one used for the analysis of conventional radial slot grain.

The pressure distribution at the exit of the forward slot for this modified grain design is presented in Fig. 6. As can be seen from this figure, there is no indication of adverse pressure gradient at the propellant surface with this grain design. The flow streamlines near the exit of the forward slot, shown in Fig. 7, demonstrate that the flowfield at the slot exit is free of any reversed flow regions. The absence of the reversed flow regions near the propellant surface should render the flow structure less susceptible to instabilities than that with the conventional radial slot design. Similarly, the pressure distribution on the propellant surface obtained with the aft-curved radial slot design should also be better from the grain deformation stand point.

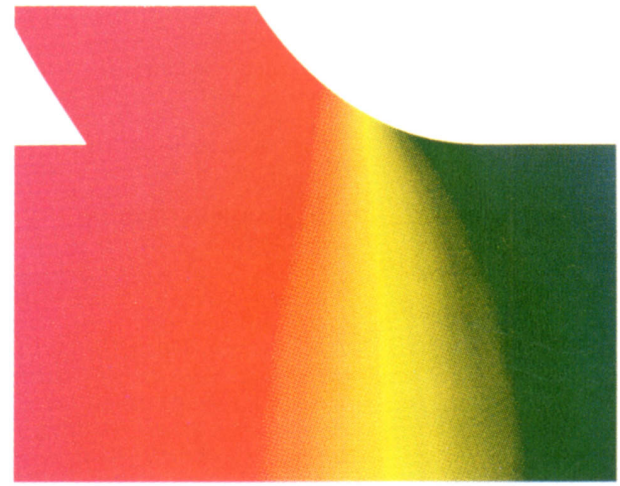

Fig. 6 Pressure distribution near forward slot exit (conventional radial slot design).

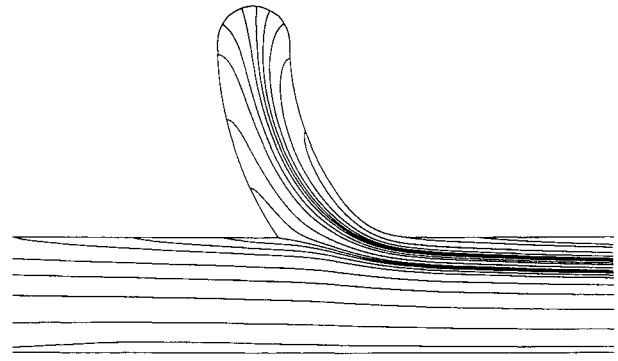

Fig. 7 Streamlines for flow near forward slot at ignition (aft-curved radial slot design).

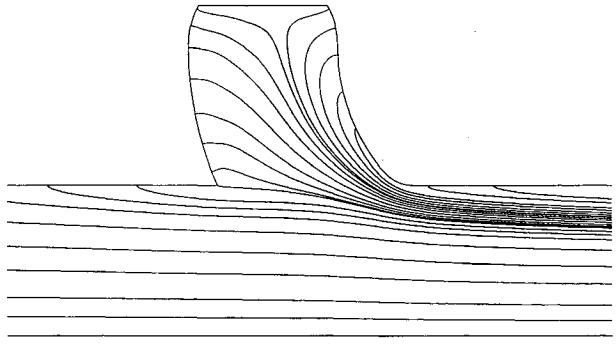

Fig. 8 Streamlines for flow near forward slot at 22% web burn (aft-curved radial slot design).

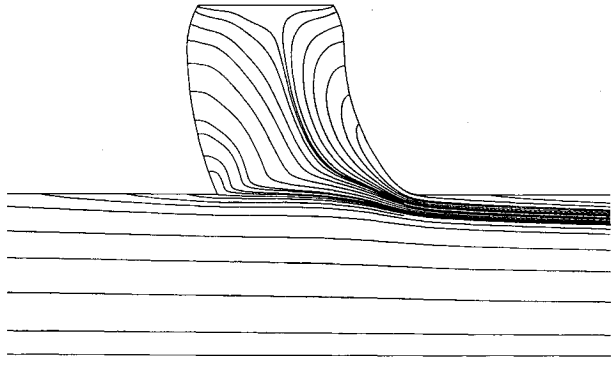

Fig. 9 Streamlines for flow near center slot at 22% web burn (aft-curved radial slot design).

The ignition condition geometry (i.e., 0% web burn) was selected for the analyses discussed previously. The reason for this choice is that the flow velocities are maximum at this time, and hence, any flow reversal is most likely to occur at this time. However, the aerodynamic surface at the aft corner with the aft-curved slot design will disappear as the propellant burns back. With the grain design considered here, the curvature at the aft edge of the slot is completely eliminated at 40% web burn. While the flow velocities at this time would be lower, it is necessary to examine the flow structure at several web burns to verify that the flow reversal is not present at some later time. The results of such a study would also be useful in identifying any other flowfield features (such as shear layers and vortices) that might be present in the motor and would influence the motor operation. Hence, the internal flow analysis for this grain design was undertaken with geometries corresponding to approximately 22, 40, and 75% web-burn conditions. The port geometries corresponding to these web-burn conditions were obtained using the industry standard Solid Propellant Rocket Motor Performance Prediction Computer Program (SPP) and used for generating the computational grids. The grain burn-back calculations included the effect of local burn rate variations caused from pressure drop and erosive burning. The computational grid for the 22 and 40% web-burn geometries was similar to the one used at the ignition geometry. For the analysis of the 75% web-burn geometry, it was necessary to increase the number of radial grid points to 90 to accommodate the necessary topological changes.

22% Web-Burn Analysis

The streamlines for the flowfield near the forward and center slots with the 22% web-burn geometry are shown in Figs. 8 and 9, respectively. These figures show that there is no indication of flow reversal developing at these locations. The streamlines for the flowfield near the aft slot for this geometry are shown in Fig. 10. As can be seen from this figure, there is no flow reversal at the slot exit, however, a vortical structure similar to that observed in a driven cavity appears in the slot cavity.

40% Web-Burn Analysis

The flow analysis for 40% web-burn geometry was undertaken to study the flow structure when the curvature at the aft edge of the slot is eliminated because of grain burn-back. The flow streamlines near the forward and the aft slots are shown in Figs. 11 and 12, respectively. As can be seen from these figures, there is no flow reversal near the slot exit. The driven-cavity-like vortex in the aft slot cavity is larger for this geometry. The flowfield in the center slot cavity was found to be similar to the forward slot and free of any flow reversal or a vortex.

75% Web-Burn Analysis

To study the evolution of the flowfield through the motor burn, analysis of the flow at 75% web-burn geometry was undertaken. The flow structure in the forward and the center slot was found to be free of any surprise at this time. The streamlines for the flowfield near the center slot are shown in Fig. 13 to illustrate this issue. The flowfield in the aft slot cavity continues to evolve as the cavity gets shallower and wider. At the 75% web-burn geometry, the flow structure re-

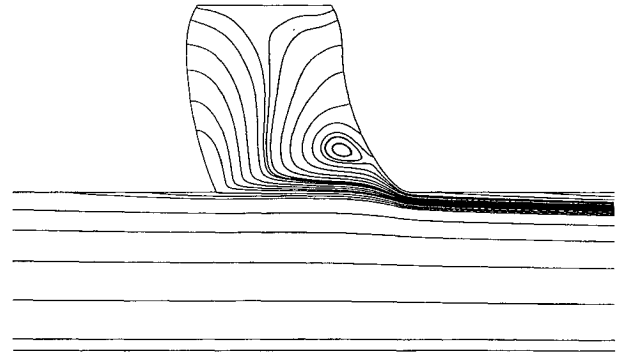

Fig. 10 Streamlines for flow near aft slot at 22% web burn (aft-curved radial slot design).

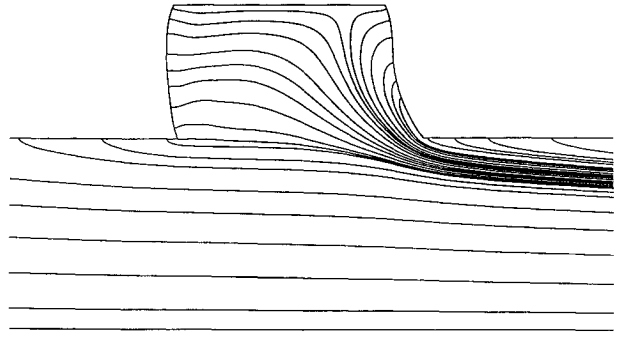

Fig. 11 Streamlines for flow near forward slot at 40% web burn (aft-curved radial slot design).

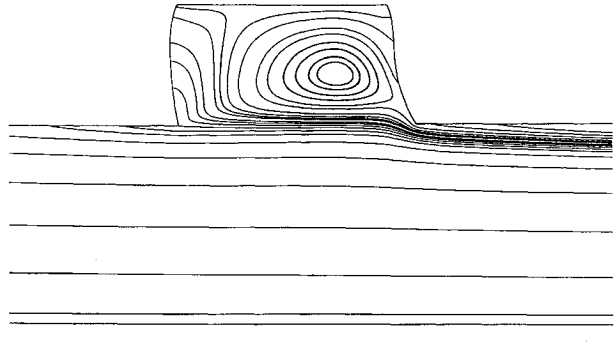

Fig. 12 Streamlines for flow near aft slot at 40% web burn (aft-curved radial slot design).

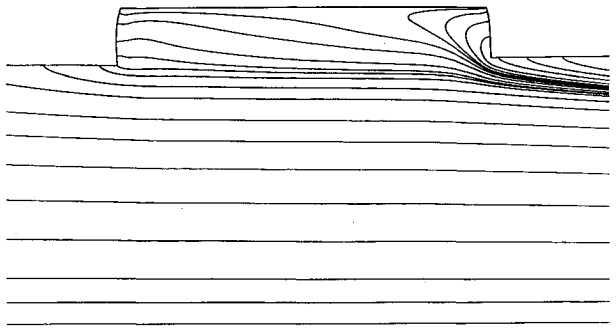

Fig. 13 Streamlines for flow near forward slot at 75% web burn (aft-curved radial slot design).

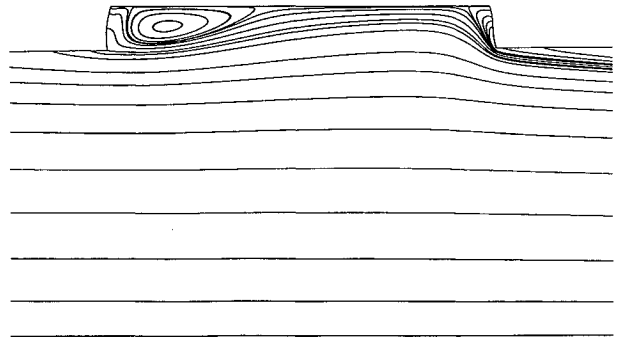

Fig. 14 Streamlines for flow near aft slot at 75% web burn (aft-curved radial slot design).

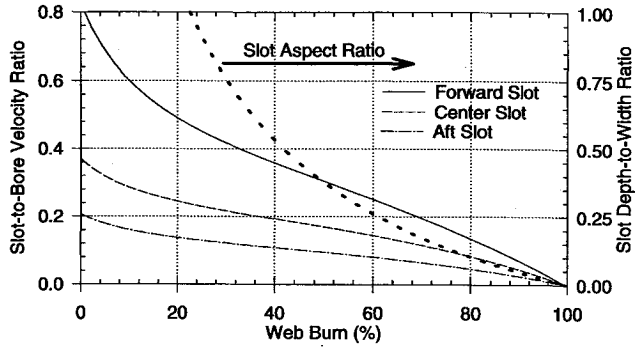

Fig. 15 Variation of slot-to-bore velocity ratio with web burn.

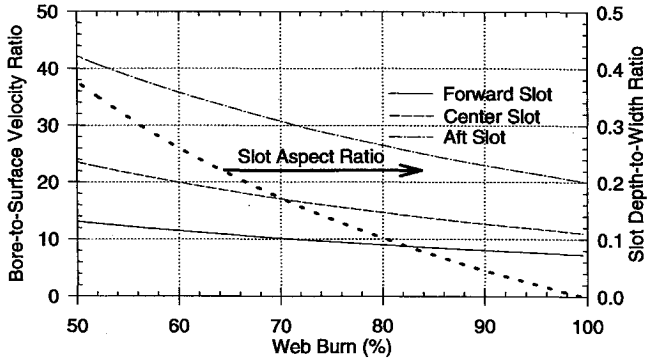

Fig. 16 Variation of bore-to-surface velocity ratio with web burn.

sembles that for the flow over a backward-facing step. The streamlines for this flowfield can be seen in Fig. 14.

Evolution of Flow Structure

The results previously discussed for the various web-burn conditions show that the flow structure in the aft slot cavity evolves into a driven-cavity-like flow, and finally into a flow similar to the flow over a backward-facing step. The flow structure in the forward and the center slot, however, undergoes no such evolution. An improved understanding of this phenomenon can be obtained by considering a simple one-dimensional model that examines the ratio of slot exit velocity to the bore flow velocity for the three slots. For a specific motor, a parameter that would determine whether or not a driven-cavity-like flow structure will exist, is a function of this velocity ratio. A driven-cavity-like flow can only be established when this ratio is sufficiently low.

Using a simple one-dimensional flow model, one can plot this ratio against web burn for the three slots. Figure 15 shows such a plot for this motor. As can be seen from this plot, the value of the slot-to-bore velocity ratio decreases with web burn. Hence, a driven-cavity-like flow can be established in a slot cavity as the web burns back. The computed results indicate that a driven-cavity-like flow exists in the forward slot when the slot-to-bore velocity ratio is about 0.13 (see the aft slot curve at 22% web burn). Hence, one would expect to see similar flow structure in the center slot cavity at 63% web burn and in the forward slot cavity at 79% web burn. However, the aspect ratio for the slot cavities plotted in Fig. 15 indicates that width-to-depth ratio for the center and the forward slot cavities at these conditions will be greater than 4 and 8, respectively. This geometry is more like a backward-facing step rather than a cavity. Hence, the forward and the center slot cavities never exhibit a driven-cavity-like flow structure in this motor.

Using similar reasoning, it can be seen that a parameter that would determine whether or not a flow structure similar to a backward-facing step flow will exist, is a function of the ratio of the bore flow velocity to the velocity normal to the forward edge of the cavity (i.e., the gas velocity at the propellant surface for this motor). The magnitude of this bore-to-surface velocity ratio needs to be sufficiently high to establish a backward-facing step flow. Figure 16 shows this ratio plotted against the web burn for the three slots. As can be seen from this figure, the bore-to-surface velocity ratio values for the forward and the center slots are significantly lower than those for the aft slot. Hence, the backward-facing flow structure can never be established at the forward and center slot cavities in this motor.

Summary

A comprehensive study of the flow structure in a solid rocket motor with radial slots was conducted using computational fluid dynamics tools. The results of the calculations were used to identify flowfield features associated with the radial slots that can adversely impact the motor operation via undesirable grain deformation and flow-induced instabilities. The flowfield structure for a modified radial slot grain design aimed at eliminating these shortcomings was also examined in detail. This design incorporates aft-curved radial slots with a contoured surface at the aft corner of the slots. This geometry provides a better aerodynamic flow-path to turn the slot flow toward the nozzle, and was found to produce a flowfield with markedly improved flow structure. The low-pressure region observed near the aft edge of conventional radial slot designs (that can result in undesirable grain deformation) is eliminated with the modified slot design. The analysis also indicates that the resulting flowfield is free of flow reversal at the propellant surface near the aft edge of the slot. This flow structure should, therefore, be less susceptible to instabilities.

The internal flow structure in the motor at several web-burn conditions was simulated. These simulations revealed that the evolution of the flow structure during the motor burn in the slot cavity is strongly influenced by the axial location of the slot. The flow structure in the aft slot cavity of the three-slot motor studied evolved to resemble a driven-cavity flow at about 22% web burn. At later burn-back geometry, the flow

in this slot evolved to resemble the flow over a backward-facing step. No similar flow structure evolution was observed in the forward and the center slots of this motor. The evolution of the flow structure is a consequence of the changes in the slot geometry as well as the flow velocity ratios as a function of the web burn (see the foregoing discussion under Evolution of Flow Structure). Useful insight into the differences between the flow structure evolution in these slot cavities can be gained by considering the variation of the slot-to-bore velocity ratio and the bore-to-surface velocity ratio with the web burn.

Acknowledgments

This research was supported under an IR&D program of United Technologies Chemical Systems Division. The authors would like to acknowledge the diligent assistance provided by Lisa Vaughn in grid generation for the computations. The first author would also like to thank G. J. Hendricks, F. E. C. Culick, J. N. Levine, and several other colleagues for their contributions to numerous discussions held during this effort.

References

[1]Glick, R. L., Caveny, L. H., and Thurman, J. L., "Internal Ballistics of Slotted-Tube Solid Propellant Rocket Motors," *Journal of Spacecraft and Rockets*, Vol. 4, No. 4, 1967, pp. 525–530.

[2]Sabnis, J. S., Gibeling, H. J., and McDonald, H., "Navier-Stokes Analysis of Solid Propellant Rocket Motor Internal Flows," *Journal of Propulsion and Power*, Vol. 5, No. 6, 1989, pp. 657–664.

[3]Chang, I., "An Efficient Solution for Viscous Flow Inside SRM," AIAA Paper 91-2429, June 1991.

[4]Madabhushi, R. K., Sabnis, J. S., De Jong, F. J., and Gibeling, H. J., "Calculation of Two-Phase Aft-Dome Flowfield in Solid Rocket Motors," *Journal of Propulsion and Power*, Vol. 7, No. 2, 1991, pp. 178–184.

[5]Golafshani, M., and Loh, H. T., "Computation of Two-Phase Viscous Flow in Solid Rocket Motors Using a Flux-Split Eulerian-Lagrangian Technique," AIAA Paper 89-2785, July 1989.

[6]Sabnis, J. S., De Jong, F. J., and Gibeling, H. J., "A Two-Phase Restricted Equilibrium Model for Combustion of Metalized Solid Propellants," AIAA Paper 92-3509, July 1992.

[7]Jones, W. P., and Launder, B. E., "The Prediction of Laminarization with a Two-Equation Model of Turbulence," *International Journal of Heat and Mass Transfer*, Vol. 15, No. 2, 1972, pp. 301–314.

[8]Sabnis, J. S., Madabhushi, R. K., Gibeling, H. J., and McDonald, H., "On the Use of k-ε Turbulence Model for Computation of Solid Rocket Internal Flows," AIAA Paper 89-2558, July 1989.

[9]Gibeling, H. J., De Jong, F. J., Sabnis, J. S., and Madabhushi, R. K., "Advanced Flow Field Model," U.S. Air Force Phillips Lab., CR PL-TR-3005, Edwards AFB, CA, March 1993.

[10]Briley, W. R., and McDonald, H., "Solution of the Multidimensional Compressible Navier-Stokes Equations by a Generalized Implicit Method," *Journal of Computational Physics*, Vol. 24, Aug. 1977, pp. 372–397.

[11]Briley, W. R., Buggeln, R. C., and McDonald, H., "Solution of the Three-Dimensional Navier-Stokes Equations for a Steady Laminar Horseshoe Vortex Flow," *Proceedings of the AIAA 7th Computational Fluid Dynamics Conference*, AIAA, New York, 1985, pp. 299–312.